
**ORDER, DISORDER, AND PHASE TRANSITION
IN CONDENSED SYSTEM**

NMR Studies of the Magnetic State of Interfacial Cobalt in (Co/Ge)_n Films

G. S. Patrin^{a,b,*}, V. K. Maltsev^a, I. N. Krayukhin^a, and I. A. Turpanov^a

^a*Kirensky Institute of Physics, Russian Academy of Sciences, Siberian Branch, Krasnoyarsk, 660036 Russia*

^b*Siberian Federal University, Krasnoyarsk, 660041 Russia*

^{*}*e-mail: patrin@iph.krasn.ru*

Received June 26, 2013

Abstract—The results of NMR studies of film structures in a cobalt–germanium system as a function of the cobalt layer thickness are presented. Two phases of cobalt, one is a face-centered cubic phase and the other is presumably a Co–Ge alloy with a weakly ferromagnetic order, have been found to exist. A “dead” layer no more than 2 nm in thickness is formed at the interface.

DOI: 10.1134/S1063776113140033

1. INTRODUCTION

The creation of multilayer magnetic films has opened new prospects for the construction of magnetic materials with specified properties. The possibility to vary the various chemical components and to change the thickness of layers and the ways of their stacking leads to a rich diversity of effects observed in these films. In recent years, layered ferromagnetic metal/semiconductor (FM/SC) structures have aroused considerable interest [1, 2]. In these systems, when a semiconductor material is used as a spacer, it becomes possible to control the properties of the spacer and interlayer coupling through external factors, such as impurities, various kinds of emissions, temperature, magnetic fields, etc.

The results obtained previously are associated to a greater extent with the investigation of systems with a silicon spacer, and certain results have been obtained here [3–5]. An increase in the number of semiconductor materials as a nonmagnetic spacer has expanded noticeably the spectrum of observed phenomena; in particular, the relationship between magnetic properties (thermomagnetic effects) and technological conditions (the material deposition rate, the substrate temperature) manifests itself in Co–Ge systems [6, 7]. It has been found that at a large thickness of the cobalt layer ($t_{\text{Co}} > 50$ nm), it has a hexagonal close-packed (hcp) structure, while at a small thickness and large deposition rates, a face-centered cubic (fcc) phase is formed. It turns out that the magnetic state of cobalt is also affected by what state the germanium spacer is in. This suggests that the interaction at the interface between two different materials affects the formation of the magnetic phase of the magnetoactive layer and the magnetic structure of the entire film. In Co/Ge films grown by molecular beam epitaxy, it has been found by the surface magnetooptic Kerr effect

(SMOKE) method that ferromagnetic order begins to form at a cobalt thickness of more than nine molecular layers [8], with the nonmagnetic layer thickness being dependent on interface roughness [9].

Since the nuclear magnetic resonance (NMR) method is sensitive to the magnetic state of cobalt and since a distinctive absorption line corresponds to each phase, we carried out a dedicated study of the change in the NMR line of ⁵⁹Co nuclei as a function of the experimental conditions and film structure.

2. SAMPLES AND THE MEASURING TECHNIQUE

The experiments were carried out on multilayer Co–Ge films. The multilayer structures were films with $n = 3–12$ pairs of cobalt and germanium. The films were grown by ion–plasma sputtering in an argon atmosphere as described in [6]. The following deposition rates were used to produce the films: 0.15 nm s^{−1} for cobalt and 0.12 ± 0.02 nm s^{−1} for germanium. Cover glasses with a temperature of 373 K during sputtering were used as substrates. The average germanium and cobalt thicknesses were determined by X-ray spectroscopy.

We investigated a series of films where the nominal thickness of germanium was fixed, $t_{\text{Ge}} = 2.0 \pm 0.3$ nm, while the thickness of cobalt was variable, $t_{\text{Co}} = 2–12$ nm. Initially a Ge buffer layer about 20 nm in thickness and subsequently the multilayer structure being investigated were deposited on the substrate, and the entire system was covered from above with a protective germanium layer about 20 nm in thickness. Check films with a definitely large thickness of the magnetic layer were also fabricated: (1) from pure Co(100 nm) and (2) a trilayer Co(88 nm)/Ge(4 nm)/Co (88 nm) structure. The NMR spectra were measured by the

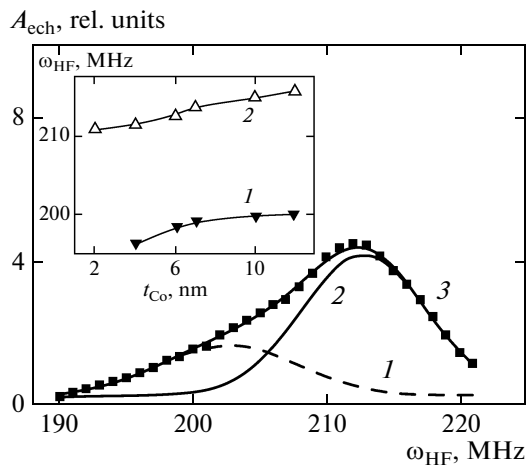


Fig. 1. Spectrum of the NMR signal for a Co(7)/Ge(2) film. 1 and 2—theoretical fits, 3—experimental data. In the inset, the resonance frequencies of lines 1 and 2 are plotted against the magnetic layer thickness in a multilayer film.

two-pulse spin-echo technique with a spectrometer that we created according to a standard scheme similar to that described in [10]. The power of the high-frequency oscillator was ~ 1 W at a receiver sensitivity of ~ 0.1 μ V, which provided a sensitivity of $\sim 10^{14}$ – 10^{15} spins in our case. The working frequency range was $\omega_{\text{HF}} = 150$ – 240 MHz. The duration of the probing high-frequency magnetic-field pulses was 0.1 – 1.0 μ s (in our experiment, we used a standard duration of about 0.2 – 0.5 μ s); the separation between them was 4 – 5 μ s. The area of the film being measured was typically ~ 1 cm^2 .

3. RESULTS AND DISCUSSION

It is well known [11] that a frequency range $\omega_{\text{hcp}} \approx 228$ MHz corresponds to the hcp phase of cobalt, central frequencies $\omega_{\text{fcc}} \approx 217.2$ MHz and $\omega_{\text{bcc}} \approx 198$ MHz correspond to the fcc and bcc phases, and the lines at $\omega_{\text{am}} < 190$ MHz, as a rule, correspond to structurally disordered phases (for example, amorphous) at a typical line width $\Delta\omega \sim 5$ – 10 MHz. For the undistorted individual phase of cobalt, the resonance line shape is Gaussian.

When investigating multilayer $(\text{Co}/\text{Ge})_n$ films, we observed a complex shape of the absorption line. We used the procedure of decomposing the experimentally obtained NMR line into its constituent Gaussian lines. Figure 1 presents a typical picture upon the absorption line decomposition. The resulting curve turned out to be well represented by a superposition of two lines: line 2 corresponds to the fcc phase and line 1 corresponds either to the bcc phase or to a disordered state. Depending on the nominal thickness of the cobalt layer, the fcc line exhibits a frequency shift from $\omega = 211$ MHz ($t_{\text{Co}} = 4$ nm) to $\omega = 216$ MHz

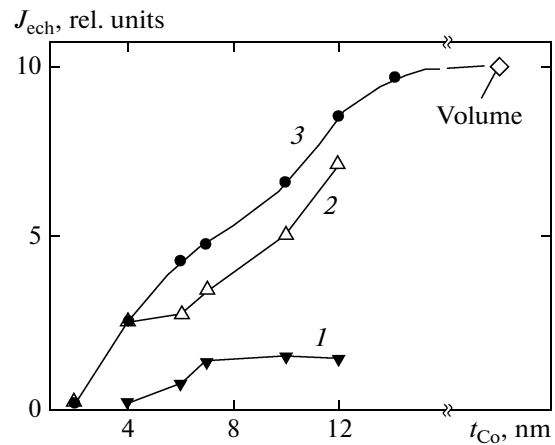


Fig. 2. Specific NMR absorption intensity versus thickness of the cobalt magnetic layer in a multilayer $(\text{Co}/\text{Ge})_n$ film: 1—additional line, 2—fcc phase, and 3—total intensity.

($t_{\text{Co}} = 12$ nm). However, all these changes occur within the absorption line width. At the same time, the position of line 1 is virtually constant (see the inset in Fig. 1). When processing the experimental data, we established that the line intensity (defined as the area under the corresponding absorption curve from a unit surface) per unit thickness of cobalt in the multilayer structure has the dependence presented in Fig. 2 irrespective of the number of pairs of layers n . It can be seen from this figure that the main NMR signal (the fcc phase) is absent at $t_{\text{Co}} < 2$ nm, while the low-field signal vanishes at $t_{\text{Co}} < 4$ nm (only a small part of this resonance curve is clearly outlined).

As is well known [12], the NMR signal intensity is proportional to the nuclear magnetization, $J_{\text{ech}} \sim I_{\text{nuc}}$, and its behavior is typical of a paramagnetic system. In magnetically ordered materials in a zero magnetic field, the nuclear subsystem is magnetized mainly through the effective field produced by the magnetization of the electronic subsystem. Thus, the position of the NMR line, its HF absorption intensity, and the temperature behavior carry information about the sample magnetization state. Since the contribution of the external fields from the environment to the local field on the nucleus is additive, a change in the coordination number will lead to a change in this field. If the elements are assumed to be mixed at the interface, then a new phase can be formed at the interface. It was established experimentally [11] that under a diamagnetic substitution in the fcc phase of cobalt, each removed magnetic atom leads to a resonance frequency shift by 16 – 18 MHz, depending on the sample quality (for example, the substitution of cobalt by Si, Cu, and Ge gives a shift of 16 MHz; see Table 2.3 in [11]). This is well described by the empirical relation $\Delta\omega \approx -\omega_{\text{fcc}}/z$, where z is the coordination number. As applied to our case, it follows that the emergence of the line at $\omega = \omega_{\text{fcc}}(11/12) \approx 199.9$ MHz in the fcc

phase can be associated with the formation of a $\text{Co}_{11}\text{Ge}_1$ alloy, which coincides rather closely with the observed line 1 of the NMR signal (about 200 MHz) in Fig. 1.

In principle, the bcc phase can be formed. According to the published data [13, 14], the bcc layer thickness does not exceed 3 nm for epitaxially grown high-quality films; a transition to the hcp phase occurs at a larger thickness. The quality and thickness of the bcc layer depend strongly both on the substrate material and temperature and on the cobalt deposition rate [15]. The bcc phase is always a strained one, but the strain should not exceed 1.6% relative to the bulk cobalt lattice parameter. In our case, the additional line 2 falls into the frequency domain of existence of the cobalt bcc phase, but this line emerges at a thickness of 4 nm. Besides, the discrepancy between the lattice constants for various atomic planes of germanium ($a_{\text{Ce}} = 0.566$ nm) and bcc cobalt ($a_{\text{bcc}} = 0.2866$ nm) exceeds the admissible value.

As can be seen from Fig. 2, the cobalt layer thickness, $t_{\text{Co}} \approx 4$ nm, is notable. For the fcc phase, the slope of the dependence $J_{\text{ech}}(t_{\text{Co}})$ changes in this region and the additional line 1 emerges. This result can be explained by the fact that when the cobalt layer is deposited on germanium, a “dead” (nonmagnetic) cobalt layer is initially formed at $t_{\text{Co}} \leq 2$ nm, which is consistent with the results from [8, 9]. As t_{Co} increases further, magnetization appears in the cobalt layer and a transition layer of a new phase is formed upon reaching $t_{\text{Co}} \approx 6$ nm. Mutual diffusion of the elements probably occurs in the range $t_{\text{Co}} \approx 4$ –6 nm. The transition layer grows to a certain limit. Once the cobalt layer has reached its critical thickness, diffusion ceases and a purely cobalt layer then begins to grow. This manifests itself as a change in the intensity of curve 2 with thickness t_{Co} in Fig. 2.

The temperature behavior of the NMR echo signal for films with different mean thicknesses of the cobalt layer differs significantly. For example, no NMR signal is observed for $(\text{Co}/\text{Ge})_n$ films with a large cobalt layer thickness, $t_{\text{Co}} \geq 12$ nm, and films of pure cobalt at nitrogen temperatures; the line rapidly broadens with decreasing temperature, and the signal becomes unobservable. For a $\text{Co}(7 \text{ nm})/\text{Ge}(2 \text{ nm})$ film, the signal intensity in nitrogen is lower than that at room temperature approximately by 30%. The magnitude of the NMR echo signal is known [12] to be inversely proportional to the magnetic anisotropy field, which depends very strongly on the strains between the substrate and film. In the literature [16], there are reports on a significant dependence of the structure and local anisotropy of cobalt films on the type of substrate and temperature in the case of deposition by molecular beam epitaxy. Note that we took no special measures to stabilize a particular phase of cobalt. In our case of the deposition of a film structure on a glass substrate and a large discrepancy between the lattice parameters of germanium and cobalt, the strain at the interface

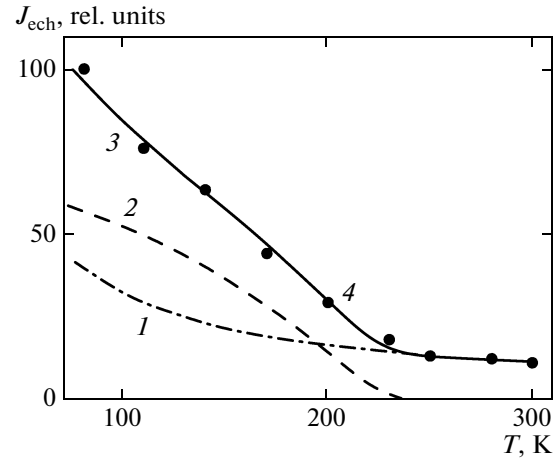


Fig. 3. Temperature dependences of the NMR signal intensity for a film with $t_{\text{Co}} = 4$ nm: 1—paramagnetic contribution from the nuclear subsystem of fcc cobalt, 2—contribution from the weakly ferromagnetic phase, 3—theoretical fit, and 4—experimental data.

should reach very high values. Therefore, the scatter of local fields on the nuclei will be significant, and this, along with the growth of the anisotropy field with decreasing temperature, will lead to a broadening of the absorption line and a “smearing” of the NMR signal, which actually is observed experimentally.

For films with a small cobalt layer thickness, where the specific weight of the new phase is considerably higher, the temperature behavior of the NMR signal differs noticeably. Figure 3 presents the temperature behavior of the signal intensity for a film with layer thicknesses $t_{\text{Co}} = 4$ nm and $t_{\text{Ge}} = 2$ nm (curve 4). It can be seen that the signal intensity begins to increase noticeably with decreasing temperature near $T_0 \sim 230$ K. Since the signal intensity is proportional to the number of absorbing centers and, accordingly, magnetization, we analyzed the temperature behavior of the possible contributions to the magnetization. Based on the fact that line 1 belongs to the fcc phase, we used the superfine splitting on the cobalt nuclei precisely for this phase ($E_{\text{sf}} = 7.243 \times 10^{13}$ erg) [17] and, having used the experimental values at temperatures $T > 250$ K, we obtained curve 1 in Fig. 3. We attempted to fit the remaining part using various model dependences. Curve 3 in Fig. 3 provides the best fit to the experimental data. It is a superposition of two dependences,

$$J_{\text{ech}} = J_{\text{para}} + J_{\text{MO}}, \quad (1)$$

where

$$J_{\text{para}} = A[\cot(E_{\text{sf}}/k_{\text{B}}T) - k_{\text{B}}T/E_{\text{sf}}] \quad (2)$$

is the paramagnetic contribution of the nuclear subsystem from the fcc phase (curve 1) (the Brillouin function, $A = 8.8 \times 10^5$), and

$$J_{\text{MO}} = B[1 - (T/T_0)^2] \quad (3)$$

is the contribution from the magnetically ordered electronic subsystem arising from the echo amplification effect [12] (curve 2). Here, k_B is the Boltzmann constant; $B = 65$ and $T = 230$ are the fit parameters. The tail near T_0 (solid curve) is obtained after the subtraction of the sum of two theoretical curves, 1 and 2, from the experimental curve 4 and is probably attributable to film inhomogeneity at a small thickness of the magnetic cobalt layer (at a thickness of less than 3 nm, the cobalt layer can have an island structure). A dependence of the temperature change in magnetization like (3), namely the quadratic dependence, is obtained in the Stoner model for weakly ferromagnetic systems of collective electrons [18]. The main mechanism leading to such a behavior stems from the fact that the system is in an unsaturated magnetic state and electron–hole spin-flip transitions occur at a small width of the Stoner gap. The theoretical results in the Stoner model are sensitive to the band structure near the Fermi level. Although such a weakly ferromagnetic behavior is believed to be unrealistic, nevertheless, such a behavior is observed experimentally in a number of cases (for example, $ZrZn_2$ and Sc_3In) [18].

Unfortunately, in the literature there are virtually no data on the magnetic properties of cobalt–germanium compounds in both film and bulk states. Among the known Co–Ge compounds [19], there are no those that could provide the required fields on the cobalt nuclei. This suggests that a new cobalt–germanium compound with weakly ferromagnetic properties is formed at the interface. Since such a behavior is not observed for bulk samples of various cobalt compounds, a new state that exists in a film state on nanosized scales has probably been detected.

ACKNOWLEDGMENTS

We thank L.A. Li for the help in preparing the films and G.V. Bondarenko for the X-ray measurements. This work was supported by the Russian Foundation for Basic Research (project no. 11-02-00675-a).

REFERENCES

1. M. R. Hofmann and M. Oestreich, in *Magnetic Heterostructures: Advances and Perspectives in Spinstructures and Spintransport*, Ed. by H. Zabel and S. D. Bader (Springer-Verlag, Berlin, 2008), Ch. 7, p. 335.
2. G. S. Patrin and V. O. Vas'kovskii, *Phys. Met. Metallogr.* **101** (Suppl. 1), S63 (2006).
3. S. Toscano, B. Briner, H. Hopster, and M. Landolt, *J. Magn. Magn. Mater.* **114**, L6 (1992).

4. J. E. Mattson, S. Kumar, E. E. Fullerton, S. R. Lee, C. H. Sowers, M. Grimsditch, S. D. Bader, and F. T. Parker, *Phys. Rev. Lett.* **71**, 185 (1993).
5. G. S. Patrin, V. O. Vas'kovskii, D. A. Velikanov, A. V. Svalov, and M. A. Panova, *Phys. Lett. A* **309**, 155 (2003).
6. G. S. Patrin, Chan-Gyu Lee, I. A. Turpanov, S. M. Zharkov, D. A. Velikanov, V. K. Maltsev, L. A. Li, and V. V. Lantsev, *J. Magn. Magn. Mater.* **306**, 218 (2006).
7. A. V. Kobayakov, G. S. Patrin, I. A. Turpanov, L. A. Li, K. G. Patrin, V. I. Yushkov, E. A. Petrakovskaya, and M. V. Rautskii, *Solid State Phenom.* **168–169**, 273 (2011).
8. J. S. Tsay, Y. T. Chen, W. C. Cheng, and Y. D. Yao, *J. Magn. Magn. Mater.* **282**, 81 (2004).
9. J. S. Tsay, H. Y. Nieh, C. S. Yang, and Y. D. Yao, *J. Magn. Magn. Mater.* **272**, e829 (2004).
10. A. S. Karnachev and E. E. Solov'ev, *Instrum. Exp. Tech.* **39** (4), 539 (1996).
11. P. C. Riedi, T. Thomson, and G. J. Tomka, in *Handbook of Magnetic Materials*, Ed. by K. H. J. Buschow (Elsevier, Amsterdam, The Netherlands, 1999), Vol. 12, p. 97.
12. M. P. Petrov, in *Physics of Magnetic Dielectrics*, Ed. by G. A. Smolenskii (Nauka, Leningrad, 1974), p. 177 [in Russian].
13. Hong Li and B. P. Tonner, *Phys. Rev. B: Condens. Matter* **40**, 10241 (1999).
14. H. Wieldraaijer, J. T. Kohlhep, P. LeClair, K. Ha, and J. M. de Jonge, *Phys. Rev. B: Condens. Matter* **67**, 224430 (2003).
15. G. A. Prinz, in *Ultrathin Magnetic Structures II: Measurement Techniques and Novel Magnetic Properties*, Ed. by B. Heinrich and J. A. C. Bland (Springer-Verlag, Berlin, 2005), p. 1.
16. H. A. M. de Gronckel, P. J. H. Bloemen, E. A. M. Van Alphen, and W. J. M. de Jonge, *Phys. Rev. B: Condens. Matter* **49**, 11327 (1994).
17. *Magnetic Properties of Metals: d-Elements, Alloys, and Compounds*, Ed. by H. P. J. Wijn (Springer-Verlag, Berlin, 1991), p. 7.
18. V. Yu. Irkhin and Yu. P. Irkhin, *Electronic Structure, Physical Properties, and Correlation Effects in d- and f-Metals and Their Compounds* (Ural Branch of the Russian Academy of Sciences, Yekaterinburg, 2004), p. 152 [in Russian].
19. V. M. Denisov, S. A. Istomin, O. I. Podkopaev, N. V. Belousova, E. A. Pastukhov, L. I. Serebryakova, and T. O. Kvasova, *Germanium, Its Compounds and Alloys* (Ural Branch of the Russian Academy of Sciences, Yekaterinburg, 2002), p. 494 [in Russian].

Translated by V. Astakhov